NeuroImage: Clinical 7 (2015) 506–517

Contents lists available at ScienceDirect

NeuroImage: Clinical

journal homepage: www.elsevier.com/locate/ynicl

Patterns of brain structural connectivity differentiate normal weight from overweight subjects

Arpana Gupta[a,b,c], Emeran A. Mayer[a,b,c,d], Claudia P. Sanmiguel[a,b,c], John D. Van Horn[f], Davis Woodworth[a,g], Benjamin M. Ellingson[a,g], Connor Fling[a], Aubrey Love[a], Kirsten Tillisch[a,b,c,e], Jennifer S. Labus[a,b,c,*]

[a]Gail and Gerald Oppenheimer Family Center for Neurobiology of Stress, Ingestive Behavior and Obesity Program (IBOP), UCLA, Los Angeles, CA, USA
[b]David Geffen School of Medicine, UCLA, Los Angeles, CA, USA
[c]Division of Digestive Diseases, UCLA, Los Angeles, CA, USA
[d]Ahmanson-Lovelace Brain Mapping Center, UCLA, Los Angeles, CA, USA
[e]Integrative Medicine, GLA VHA, UCLA, Los Angeles, CA, USA
[f]The Institute for Neuroimaging and Informatics, Keck School of Medicine, USC, Los Angeles, CA, USA
[g]Radiology, David Geffen School of Medicine, UCLA, Los Angeles, CA, USA

ARTICLE INFO

Available online 13 January 2015

Keywords:
Obesity
Overweight
Morphological gray-matter
Anatomical white-matter connectivity
Reward network
Multivariate analysis
Classification algorithm

ABSTRACT

Background: Alterations in the hedonic component of ingestive behaviors have been implicated as a possible risk factor in the pathophysiology of overweight and obese individuals. Neuroimaging evidence from individuals with increasing body mass index suggests structural, functional, and neurochemical alterations in the extended reward network and associated networks.
Aim: To apply a multivariate pattern analysis to distinguish normal weight and overweight subjects based on gray and white-matter measurements.
Methods: Structural images ($N = 120$, overweight $N = 63$) and diffusion tensor images (DTI) ($N = 60$, overweight $N = 30$) were obtained from healthy control subjects. For the total sample the mean age for the overweight group (females = 32, males = 31) was 28.77 years (SD = 9.76) and for the normal weight group (females = 32, males = 25) was 27.13 years (SD = 9.62). Regional segmentation and parcellation of the brain images was performed using Freesurfer. Deterministic tractography was performed to measure the normalized fiber density between regions. A multivariate pattern analysis approach was used to examine whether brain measures can distinguish overweight from normal weight individuals.
Results: 1. White-matter classification: The classification algorithm, based on 2 signatures with 17 regional connections, achieved 97% accuracy in discriminating overweight individuals from normal weight individuals. For both brain signatures, greater connectivity as indexed by increased fiber density was observed in overweight compared to normal weight between the reward network regions and regions of the executive control, emotional arousal, and somatosensory networks. In contrast, the opposite pattern (decreased fiber density) was found between ventromedial prefrontal cortex and the anterior insula, and between thalamus and executive control network regions. 2. Gray-matter classification: The classification algorithm, based on 2 signatures with 42 morphological features, achieved 69% accuracy in discriminating overweight from normal weight. In both brain signatures regions of the reward, salience, executive control and emotional arousal networks were associated with *lower* morphological values in overweight individuals compared to normal weight individuals, while the opposite pattern was seen for regions of the somatosensory network.
Conclusions: 1. An increased BMI (i.e., overweight subjects) is associated with distinct changes in gray-matter and fiber density of the brain. 2. Classification algorithms based on white-matter connectivity

Abbreviations: HC, healthy control; BMI, body mass index; HAD, hospital anxiety and Depression Scale; TR, repetition time; TE, echo time; FA, flip angle; GLM, general linear model; DWI, diffusion-weighted MRIs; FOV, field of view; GMV, gray matter volume; SA, surface area; CT, cortical thickness; MC, mean curvature; DTI, diffusion tensor imaging; FACT, fiber assignment by continuous tracking; SPSS, statistical package for the social sciences; ANOVA, analysis of variance; FDR, false-discovery rate; sPLS-DA, sparse partial least squares for discrimination Analysis; VIP, variable importance in projection; PPV, positive predictive value; NPV, negative predictive value; VTA, ventral tegmental area; OFG, orbitofrontal gyrus; PPC, posterior parietal cortex; dlPFC, dorsolateral prefrontal cortex; vmPFC, ventromedial prefrontal cortex; aMCC, anterior mid cingulate cortex; sgACC, subgenual anterior cingulate cortex; ACC, anterior cingulate cortex

* Corresponding author at: Gail and Gerald Oppenheimer Family Center for Neurobiology of Stress, Division of Digestive Diseases, David School of Medicine at UCLA, CHS 42-210, MC737818, 10833 Le Conte Avenue, Los Angeles, CA, USA.
E-mail address: jlabus@ucla.edu (J.S. Labus).

http://dx.doi.org/10.1016/j.nicl.2015.01.005

involving regions of the reward and associated networks can identify specific targets for mechanistic studies and future drug development aimed at abnormal ingestive behavior and in overweight/obesity.

1.0. Introduction

The World Health Organization estimates that almost half a billion adults are obese and more than twice as many adults are overweight, contributing to the increase in diseases such as diabetes, cardiovascular disease, and cancer, and leading to the death of at least 2.8 million individuals every year (World Health Organization (WHO), 2014). In America alone, up to 34.9% adults are obese and twice as many adults (65%) are either overweight or obese (Center for Disease Control (CDC), 2014). The economic and health burden of being overweight and obese continues to raise health care costs to as high as $78.5 billion (Finkelstein et al., 2009), and billions of dollars continue to be spent on ineffective treatments and interventions (Loveman et al., 2011; Terranova et al., 2012). Despite various efforts directed towards identifying the underlying pathophysiology of overweight and obesity, the current understanding remains insufficient.

Both environmental and genetic factors play a role in the development of humans being overweight and obese (Calton and Vaisse, 2009; Choquet and Meyre, 2011; Dubois et al., 2012; El-Sayed Moustafa and Froguel, 2013). Recent neuroimaging studies have shown that higher body mass index (BMI) is associated with alterations in functional (task and resting state) (Connolly et al., 2013; Garcia-Garcia et al., 2013; Kilpatrick et al., 2014; Kullmann et al., 2012), gray-matter morphometry (Kurth et al., 2013; Raji et al., 2010), and white-matter properties (Shott et al., 2014; Stanek et al., 2011), suggesting a possible role of the brain in the pathophysiology of overweight and obesity (Das, 2010). These studies largely implicate regions of the reward network (Kenny, 2011; Volkow et al., 2004; Volkow et al., 2008; Volkow et al., 2011), and three closely linked networks related to salience (Garcia-Garcia et al., 2013; Morrow et al., 2011; Seeley et al., 2007a), executive control (Seeley et al., 2007b), and emotional arousal (Menon and Uddin, 2010; Zald, 2003) (Fig. 1).

The current study aimed to test the general hypothesis that interactions between regions of these networks differ between overweight individuals compared to normal weight individuals, and we applied large-scale state-of-the-art neuroimaging data processing, visualization and multivariate pattern analysis to test this hypothesis. The availability of more efficient and computationally intensive data processing pipelines and statistical algorithms allows for a more broad morphological and anatomical characterization of the brain in individuals with elevated BMIs compared to individuals with normal weight. Multivariate pattern classification analysis provides the means to examine the distributed pattern of regions that discriminate overweight compared to normal weight individuals.

In this study, a supervised learning algorithm is applied to measures of regional brain morphometry and white-matter fiber density (a measure of connectivity between specific brain regions) to test the hypothesis that overweight status is associated with distinct patterns or brain signatures comprising regions of the reward, salience, executive control, and emotional arousal networks. Results suggest that regional connectivity, and less so brain morphometrics, can be used to discriminate overweight compared to normal weight individuals. The results provide

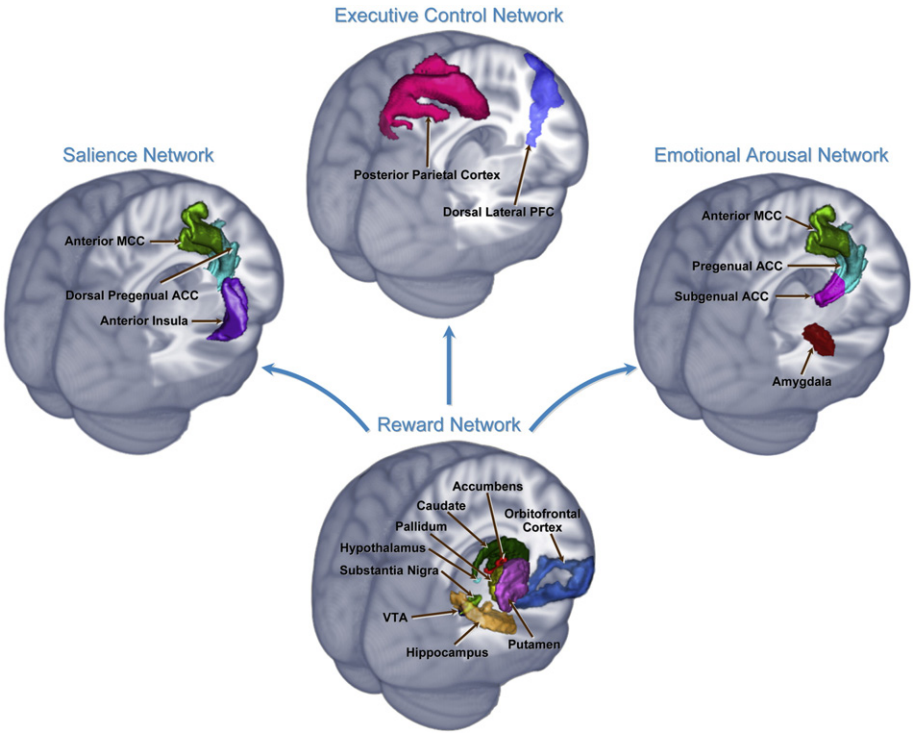

Fig. 1. Regions of the reward network and associated networks. 1. *Reward network*: hypothalamus, orbitofrontal cortex (OFC), nucleus accumbens, putamen, ventral tegmental area (VTA), substantia nigra, midbrain regions (caudate, pallidum, hippocampus). 2. *Salience network*: anterior insula, dorsal pregenual anterior cingulate cortex (dorsal pgACC), anterior mid cingulate cortex (aMCC). 3. *Executive control network*: posterior parietal cortex (PPC), dorsal lateral prefrontal cortex (dlPFC). 4. *Emotional arousal network*: pregenual anterior cingulate cortex (pgACC), subgenual anterior cingulate cortex (sgACC), anterior mid cingulate cortex (aMCC), amygdala.

a predictive algorithm based on multimodal brain imaging and identify specific targets for further mechanistic investigations.

2.0. Methods

2.1. Participants

The total sample was composed of 120 right-handed healthy control (HC) volunteers enrolled in neuroimaging studies at the Center for Neurobiology of Stress between 2010 and 2014. Subjects were recruited through advertisements posted in the UCLA and Los Angeles community. All procedures complied with the principles of the Declaration of Helsinki and were approved by the Institutional Review Board at UCLA (approval numbers 11-000069 and 12-001802). All subjects provided written informed consent. All subjects were classified as healthy after a clinical assessment that included a modified Mini-International Neuropsychiatric Interview Plus 5.0 (Sheehan et al., 1998). Exclusion criteria included substance abuse, pregnancy, tobacco dependence, abdominal surgery, vascular risk factors, weight loss surgery, excessive exercise (more than 1 h every day and marathon runners) or psychiatric illness. Even though often associated with increased BMI, subjects with hypertension, diabetes or metabolic syndrome were excluded to reduce heterogeneity of the population. Also, subjects with eating disorders, including digestive or eating disorders such as anorexia or bulimia nervosa were excluded for the same reason. Even though a BMI = 25–29.9 is considered overweight, in our study it was identified as the high BMI group. Normal weight subjects were recruited at a BMI < 25, and in our study was identified as the normal BMI group. No subjects exceeded 400 lb due to MRI scanning weight limits.

2.2. Sample characteristics

Validated questionnaires were completed before scanning and were used to measure current anxiety and depression symptoms (Hospital Anxiety and Depression Scale (HAD)) (Zigmond and Snaith, 1983). The HAD scale is a self-assessment 14-item scale that assesses current anxiety and depression symptoms in subjects at baseline (Zigmond and Snaith, 1983). In addition, the subjects had previously undergone a structured psychiatric interview (Mini International Neuropsychiatric Interview, MINI) to measure past or current psychiatric illness (Sheehan et al., 1998).

2.3. fMRI acquisition

2.3.1. Structural (gray-matter) MRI

Subjects ($N = 120$, high BMI $N = 63$) were scanned on a 3.0 Tesla Siemens TRIO after a sagittal scout was used to position the head. Structural scans were obtained from 4 different acquisition sequences using a high-resolution 3-dimensional T1-weighted, sagittal magnetization-prepared rapid gradient echo (MP-RAGE) protocol and scanning details are: 1. Repetition time (TR) = 2200 ms, echo time (TE) = 3.26 ms, flip angle (FA) = 9, 1 mm^3 voxel size. 2. TR = 2200 ms, TE = 3.26 ms, FA = 20, 1 mm^3 voxel size. 3. TR = 20 ms, TE = 3 ms, FA = 25, 1 mm^3 voxel size. 4. TR = 2300 ms, TE = 2.85 ms, FA = 9, 1 mm^3 voxel size. Influence of acquisition protocol on differences in total gray matter volume (TGMV) was assessed. Specifically the general linear model (GLM) was applied to determine protocol influences on TGMV controlling for age. Results indicated that all protocols were not similar to each other ($F(3) = 6.333$, $p = .053$).

2.3.2. Anatomical connectivity (white-matter) MRI

A subset of the original sample ($N = 60$, high BMI $N = 30$) underwent diffusion-weighted MRIs (DWIs) according to two comparable acquisition protocols. Specifically, DWIs were acquired in either 61 or 64 noncollinear directions with $b = 1000$ s/mm^2, with 8 or 1 $b = 0$ s/mm^2 images, respectively. Both protocols had a TR = 9400 ms, TE = 83 ms, and field of view (FOV) = 256 mm with an acquisition matrix of 128 × 128, and a slice thickness of 2 mm to produce $2 \times 2 \times 2$ mm^3 isotropic voxels.

2.4. fMRI processing

2.4.1. Structural (gray-matter) segmentation and parcellation

T1-image segmentation and regional parcellation were conducted using FreeSurfer (Dale et al., 1999; Fischl et al., 1999, 2002) following the nomenclature described in Destrieux et al. (2010). For each cerebral hemisphere, a set of 74 bilateral cortical structures were labeled in addition to 7 subcortical structures and the cerebellum. Segmentation results from a sample subject are shown in Fig. 2A. One additional midline structure (the brain stem which includes parts of the midbrain such as the ventral tegmental area [VTA] and the substantia nigra) was also included, for a complete set of 165 parcellations for the entire brain. Four representative morphological measures were computed for each cortical parcellation: gray matter volume (GMV), surface area (SA), cortical thickness (CT), and mean curvature (MC). Data processing workflows were designed and implemented at the Laboratory of Neuroimaging (LONI) Pipeline (http://pipeline.loni.usc.edu).

2.4.2. Anatomical connectivity (white-matter)

Diffusion weighted images (DWI) were corrected for motion and used to compute diffusion tensors that were rotationally re-oriented at each voxel. The diffusion tensor images were realigned based on trilinear interpolation of log-transformed tensors as described in Chiang et al. (Chiang et al., 2011) and resampled to an isotropic voxel resolution ($2 \times 2 \times 2$ mm^3). Data processing workflows were created using the LONI pipeline.

White matter connectivity for each subject was estimated between the 165 brain regions identified on structural images (Fig. 2B) using DTI fiber tractography. Tractography was performed via the Fiber Assignment by Continuous Tracking (FACT) algorithm (Mori et al., 1999) using TrackVis (http://trackvis.org) (Irimia et al., 2012). The final estimate of white matter connectivity between each of the brain regions was determined based on the number of fiber tracts intersecting each region, normalized by the total number of fiber tracts within the entire brain. This information was then used for subsequent classification.

2.5. Sparse partial least squares — discriminate analysis (sPLS-DA)

In order to determine whether brain markers can be used to predict high BMI status (overweight vs. normal weight) we employed sPLS-DA. sPLS-DA is a form of sparse PLS regression but the response variable is categorical, indicating group membership (Lê Cao, 2008a; Lê Cao et al., 2009b, 2011). sPLS-DA has been shown to be particularly effective with a large number of predictors, small sample size, and high colinearity among predictors (Lê Cao, 2008a; Lê Cao et al., 2009b, 2011). sPLS maximizes the sample covariance between the brain measures and a group difference contrast. sPLS simultaneously performs variable selection and classification using lasso penalization (Lê Cao et al., 2009a). sPLS-DA operates using a supervised framework forming linear combinations of the predictors based on class membership. sPLS-DA reduces the dimensionality of the data by finding a set of orthogonal components each comprised by a selected set of features or variables. The components are referred to as brain signatures. Each variable comprising a brain signature has an associated “loading”, which is a measure of the relative importance of the variables for the discrimination into the two groups (Lê Cao et al., 2008b). In addition, Variable Importance in Projection (VIP) scores were calculated in order to estimate the importance of each variable used in the PLS model. The VIP score is a weighted sum of the loadings, which takes into account the explained variance of each signature. The averaged of the squared VIP scores is equal to 1. Predictors with VIP coefficients greater than one are considered particularly important for the classification (Lê Cao et al., 2008b).

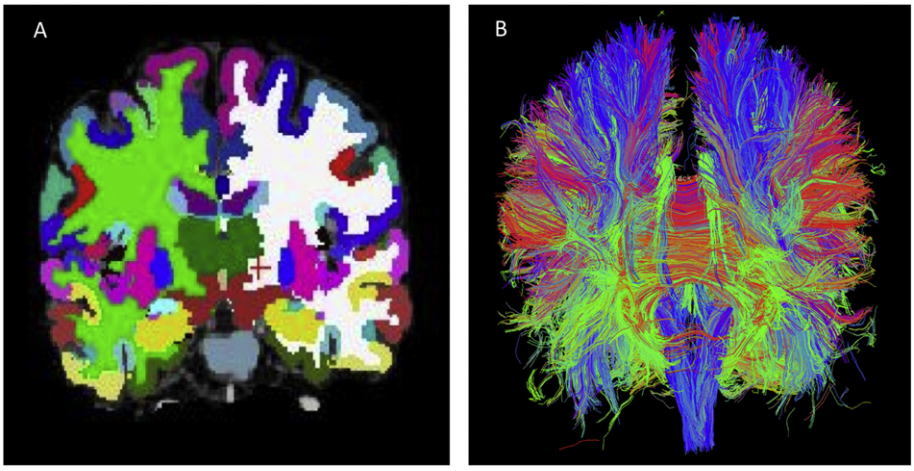

Fig. 2. A. Structural segmentation and parcellation results and B. white-matter fiber results associated with structural parcellations from a sample subject. A: Structural segmentation. B: White-matter segmentation.

2.5.1. Development of the predictive model

The number of brain signatures for each analysis was fixed at two (Lê Cao et al., 2008b). A *stability analysis* was used in order to determine the optimal number of brain regions for each brain signature (Lê Cao et al., 2011). First, sPLS-DA is applied across a range of variables, 5–200, to be selected for each of the two brain signatures. For each specification of the number of variables to select, 10-fold cross-validation repeated 100 times is performed. This cross-validation procedure divides the training data into 10 folds or subsamples of data ($n = 12$ test sets). A single subsample is set aside as test data and the remaining subsamples are used to train the model. Stability of the variables is determined by calculating the number of times a specific variable is selected across all cross-validation runs. Only brain variables with a stability of greater than 80% were used to develop the final model.

2.6. Statistical analyses

2.6.1. Sparse partial least squares — discriminate analysis (sPLS-DA)

sPLS-DA was performed using the R package mixOmics (http://www.R-project.org). We examined the predictive power of brain morphometry and DTI anatomical connectivity separately. In addition to regional brain morphometry or regional anatomical connectivity, age, and total GMV were included as possible predictors. For morphological data obtained, measures of GMV, SA, CT, and MC were entered into the model. For DTI anatomical connectivity data obtained, subject-specific matrices indexing relative fiber density between the 165 regions were transformed to 1 dimensional matrices containing 13,530 unique connectivities (upper triangle from the initial matrix). These matrices were then concatenated across subjects and entered into the sPLS-DA. As an initial data reduction step, near zero variance predictors were dropped and this resulted in 369 remaining connections. The brain signatures were summarized using variable loadings on the individual dimensions and VIP coefficients. We also use graphical displays to illustrate the discriminative abilities of the algorithms (Lê Cao et al., 2011). The predictive ability of the final models was assessed using leave one out cross-validation. We also calculated binary classification measures: sensitivity, specificity, positive predictive value (PPV) and negative predictive value (NPV). Here, the sensitivity indexes the ability of the classification algorithm to correctly identify overweight individuals. Specificity reflects the ability of the classification algorithm to correctly identify normal weight individuals. PPV reflects the proportion of the sample showing the specific overweight brain signature from the classification algorithm and who are actually overweight (true positive). On the other hand NPV is the probability that if the test result is negative, i.e., the participant does not have the overweight-specific brain signature (true negative).

2.6.2. Sample characteristics

Statistical analyses were performed using Statistical Package for the Social Sciences (SPSS) software (version 19). Group differences in behavioral measure scores were evaluated by applying analysis of variance (ANOVA). Significance was considered at $p < .05$ uncorrected.

3.0. Results

3.1. Sample characteristics

The total sample ($N = 120$) included 63 overweight individuals (females = 32, males = 31), mean age = 28.77 years, SD = 9.76, and 57 normal weight individuals (females = 32, males = 25), mean age = 27.13 years, SD = 9.62. Although the overweight group tended to have higher levels of anxiety and depression, there were no significant group differences ($F = .642$, $p = .425$; $F = .001$, $p = .980$). Clinical characteristics of the sample are summarized in Table 1.

3.2. Multivariate pattern analyses using sPLS-DA

3.2.1. Anatomical connectivity (white-matter) based classification

We examined whether brain anatomical connectivity white-matter could be used to discriminate overweight individuals from normal weight individuals. Fig. 3A depicts the individuals from the sample represented in relationship to the two brain signatures and depicts the discriminative abilities of the white matter classifier. Binary

Table 1
Sample characteristics.

	Overweight		Normal weight		Overweight vs. normal weight	
	Female	Male	Female	Male		
N	32	31	32	25		
	Mean	SD	Mean	SD	*F*	Sig
Age (years)	28.77	9.76	27.13	9.62	4.067	.056
BMI	29.60	1.13	22.05	1.52	178.541	1.65^{-6**}
HAD anxiety	3.27	2.27	2.38	2.72	.642	.425
HAD depression	1.23	1.48	1.13	1.36	.001	.980

Questionnaires: BMI, body mass index; hospital anxiety and depression (HAD anxiety), Hospital anxiety and depression (HAD depression). Subject number (*N*), Standard deviation (SD). Sig = $p < 0.05^{*}$, $p < 0.005^{**}$.

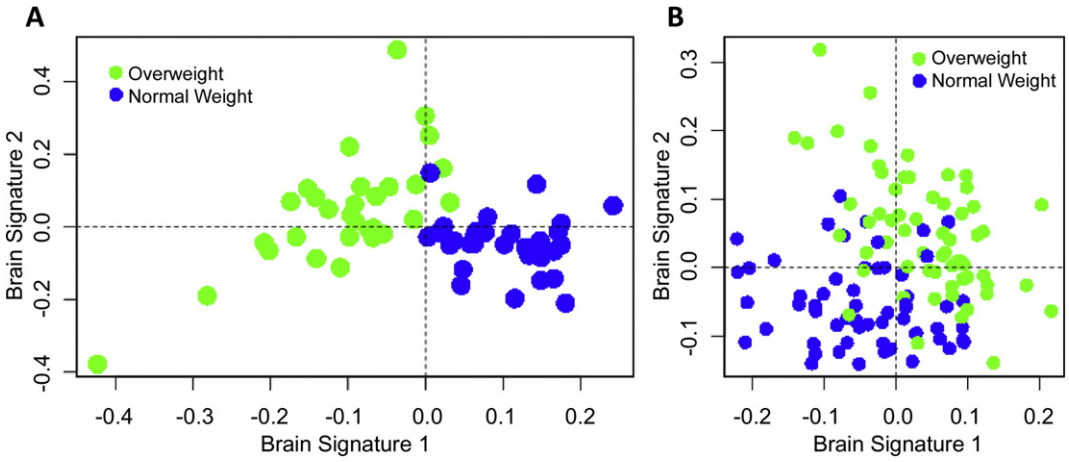

Fig. 3. A. Classifier based on fiber density (white-matter). B. Classifier based on gray-matter morphology. A: Depicts the discriminative abilities of the fiber density (white-matter) classifier. B: Depicts the discriminative abilities of the gray-matter classifier.

classification measures were calculated and indicated a sensitivity of 97%, specificity of 87%, PPV of 88%, and NPV of 96%. Table 2 contains the list of the stable white-matter connections comprising each discriminatory brain signature along with variable loadings and VIP coefficients.

3.2.2. Anatomical connectivity based brain signature 1

The first brain signature accounts for 63% of the variance. As indicated by the VIP coefficients, the variables in the solution explaining the most variance included 1) connections between regions of the reward network (putamen, pallidum, brainstem [including midbrain regions such as the VTA and substantia nigra]) with regions of the executive control (precuneus which is part of the posterior parietal cortex), salience (anterior insula), emotional arousal (ventromedial prefrontal cortex) and somatosensory (postcentral gyrus) networks; 2) regions of the emotional arousal network (anterior midcingulate cortex, ventromedial prefrontal cortex) with regions of the salience (anterior insula) and somatosensory (paracentral lobule including supplementary motor cortex) networks; and 3) thalamus with the middle occipital gyrus and thalamus with an executive control network region (dorsal lateral prefrontal cortex).

Compared to the normal weight group, the overweight group showed greater connectivity from regions of the reward network (putamen, pallidum, brainstem) to the executive control network (posterior parietal cortex), and from putamen to an inhibitory part of the emotional arousal network (ventromedial prefrontal cortex) and to regions of the somatosensory network (postcentral gyrus and posterior insula). Lower connectivity was observed in the overweight group in regions from the emotional arousal network (ventromedial prefrontal cortex) to the salience network (anterior insula), but greater connectivity in the overweight group from regions from the emotional arousal network (ventromedial prefrontal cortex) to the somatosensory network (posterior insula). Lower connectivity was also observed in the overweight group in the connections from the somatosensory (paracentral lobule) to the anterior midcingulate cortex but higher connectivity from the paracentral lobule to the subparietal sulcus (part of the somatosensory network). Looking at thalamic connections, lower connectivity was observed from the thalamus to the dorsal lateral prefrontal cortex (executive control network) and to the middle occipital gyrus in overweight individuals compared to normal weight individuals.

3.2.3. Anatomical connectivity based brain signature 2

The second anatomical brain signature identified accounted for an additional 12% of the variance in the data. The variables contributing the most variance to the group discrimination as indicated by the VIP coefficient included connections in regions of the reward (putamen, orbital sulci which is part of the orbital frontal gyrus, and brainstem) and emotional arousal (gyrus rectus which is the medial part of the ventromedial prefrontal cortex) networks.

In overweight individuals compared to normal weight individuals, greater connectivity was observed between the reward network regions (brainstem and putamen) to both the executive control (dorsal lateral prefrontal cortex) and inhibitory part of the emotional arousal (ventromedial prefrontal cortex). However, connectivity between the occipital the orbital frontal gyrus (reward network) was lower in overweight individuals compared to normal weight individuals.

3.2.4. Morphometric gray-matter based classification

We examined whether brain morphometry (gray matter volume, surface area, cortical thickness, and mean curvature) could be used to discriminate overweight individuals from normal weight individuals. Fig. 3B depicts the individuals from the sample represented in relationship to the two brain signatures and depicts the discriminative abilities of the morphometric classifier. Binary classification measures were calculated and indicated a sensitivity of 69%, specificity of 63%, PPV of 66%, and NPV of 66%. Table 3 contains the list of morphometric measures comprising each discriminative along with variable loadings and VIP coefficients.

3.2.5. Morphological based brain signature 1

The first brain signature explained 23% of the variability in the morphometric phenotype data. As seen by the VIP coefficients, variables contributing the most variance to the signature included regions of the reward (subregions of the orbital frontal gyrus), salience (anterior insula), executive control (dorsal lateral prefrontal cortex), emotional arousal (ventromedial prefrontal cortex) and somatosensory (precentral sulcus, supramarginal gyrus, subcentral sulcus, superior frontal sulcus) networks. High VIP coefficients were also observed for the superior frontal gyrus and sulcus, superior temporal gyrus, transverse frontopolar gyri, and anterior transverse temporal gyrus. Regions of the reward, salience, executive control and emotional arousal networks were associated with *lower* values in overweight individuals compared to normal weight individuals. Also, overweight individuals compared to normal weight individuals had *greater* values in regions of the somatosensory network. Morphometry of frontal and temporal regions (superior temporal gyrus, and anterior transverse temporal gyrus) were also associated with *lower* values in overweight individuals compared to normal weight individuals.

3.2.6. Morphological based brain signature 2

The second morphological brain signature explained 32% of the variance. Variables with the highest VIP coefficients were similar to the VIP

Table 2
List of anatomical connections comprising each discriminative brain signature.

Region A	Region B	LOADINGS Comp 1	LOADINGS Comp 2	VIP Comp 1	VIP Comp 2
Brain signature 1					
R Putamen	R Precuneus (part of PPC)	−0.35		1.42	1.25
R Pallidum	R Precuneus (part of PPC)	−0.29		1.20	1.06
Brain–stem (contains parts of the midbrain)	L Superior parietal lobule	−0.23		0.97	0.85
L Putamen	L Orbital part of the inferior frontal gyrus (part of vmPFC)	−0.16		0.67	0.59
R Putamen	R Postcentral gyrus	−0.28		1.14	1.00
L Putamen	L Long insular gyrus (posterior insula)	−0.24		0.98	0.86
L Inferior frontal gyrus (part of vmPFC)	L Anterior segment of the insula (anterior insula)	0.25		1.03	0.90
R Inferior frontal gyrus (part of vmPFC)	R Posterior ramus (lateral sulcus) (posterior insula)	−0.20		0.83	0.73
L Paracentral lobule	L Middle–anterior part of the cingulate gyrus (aMCC)	0.18		0.74	0.65
L Paracentral lobule	R Subparietal sulcus	−0.18		0.75	0.66
R Thalamus	R Middle frontal gyrus (part of dlPFC)	0.25		1.03	0.91
R Thalamus	R Middle occipital gyrus	0.39		1.63	1.43
R Cuneus	R Parieto–occipital sulcus	−0.33		1.37	1.20
R Occipital pole	R Middle occipital sulcus	0.29		1.20	1.06
Brain signature 2					
Brain–stem (contains parts of the midbrain)	L Angular gyrus (part of PPC)		−0.30		0.59
R Putamen	L Gyrus rectus (part of vmPFC)		−0.74		1.45
R Middle occipital gyrus	R Orbital sulci (part of OFG)		0.61		1.20

	Reward network
	Salience network
	Executive control network
	Emotional arousal
	Somatosensory network
	Thalamus
	Other (Regions not part of the reward, salience, executive control, emotional arousal, or somatosensory networks)

Abbreviations: Hemisphere: L, left, R, right; Comp1: component 1; Comp2: component 2. Regions: PPC, posterior parietal cortex; vmPFC, ventromedial prefrontal cortex; dlPFC, dorsal lateral prefrontal cortex; aMCC, anterior mid cingulate cortex; OFG, orbital frontal gyrus.
Connections are bidirectional from Region A to Region B.
The components are referred to as brain signatures.
Loading is the measure of relative importance of the variables for the discrimination into the two groups for each brain signature.
Negative loadings for each component are associated with greater connectivity in the overweight group compared to the normal weight group.
Positive loadings for each component are associated with lower connectivity in the overweight group compared to the normal weight group.
Variable importance in projection (VIP) is a weighted sum of the loadings, which takes into account the explained variance of each brain signature.
[a]Reward network.
[b]Salience network.
[c]Executive control network.
[d]Emotional arousal.
[e]Somatosensory network.
[f]Thalamus.
[g]Other (regions not part of the reward, salience, executive control, emotional arousal, or somatosensory networks).

Table 3
Regional morphometry comprising each brain signature.

Brain Region	Hemisphere	Morphometry Metric	LOADINGS Comp 1	LOADINGS Comp 2	VIP Comp 1	VIP Comp 2
Brain Signature 1						
Orbital gyri (part of OFG)	L	V	0.36		2.33	1.69
Frontopolar gyri (part of OFG)	L	CT	0.22		1.44	1.01
Orbital sulci (part of OFG)	R	V	0.15		1.01	0.96
Anterior segment of the lateral sulcus (anterior insula)	R	V	0.34		2.24	1.52
Middle frontal gyrus (part of dlPFC)	R	V	0.26		1.71	1.11
Middle frontal gyrus (Part of dlPFC)	R	SA	0.25		1.66	0.98
Inferior frontal gyrus (part of vmPFC)	L	V	0.19		1.26	0.92
Gyrus rectus (part of vmPFC)	L	V	0.19		1.22	0.93
Inferior precentral sulcus	R	SA	−0.21		1.38	1.05
Supramarginal gyrus	R	CT	−0.20		1.29	0.91
Superior frontal sulcus	R	SA	−0.17		1.13	0.68
Subcentral gyrus	L	CT	−0.15		0.96	0.41
Supramarginal gyrus	L	SA	−0.14		0.93	0.39
Inferior precentral sulcus	R	V	−0.14		0.93	0.38
Sulcus intermedius primus	L	V	−0.15		1.02	0.67
Superior frontal gyrus	R	CT	−0.18		1.15	0.72
Transverse frontopolar gyri (part of frontal pole)	R	CT	−0.23		1.53	0.73
Superior temporal gyrus	L	SA	−0.29		1.91	0.79
Anterior transverse temporal gyrus	R	SA	−0.27		1.80	0.94
Superior temporal gyrus	L	CT	−0.14		0.90	0.47
Cerebellum	L	V	−0.14		0.93	0.77
Brain signature 2						
Caudate	R	V		0.09		0.47
Anterior segment of the lateral sulcus of the insula (anterior insula)	L	V		0.25		1.26
Anterior segment of the lateral sulcus (anterior insula)	L	MC		0.16		0.81
Short insular gyri (anterior insula)	R	MC		0.14		0.72
Anterior segment of the lateral sulcus (anterior insula)	L	V		0.14		0.72
Horizontal ramus of anterior segment of the lateral sulcus (anterior insula)	L	SA		0.12		.60
Short insular gyri (anterior insula)	L	V		0.04		0.20
Precuneus (part of PPC)	L	V		0.35		1.77
Precuneus (part of PPC)	R	V		0.17		0.84

Table 3 (*continued*)

Subcallosal area (part of sgACC)	L	CT		0.33		1.67
Parahippocampal gyrus	R	SA		0.27		1.34
Anterior cingulate gyrus (ACC)	R	V		0.21		1.03
Parahippocampal gyrus	R	V		0.14		0.72
Pericallosal sulcus	R	V		0.11		0.55
Long insular gyrus (posterior insula)	R	V		−0.49		2.45
Long insular gyrus (posterior insula)	L	V		−0.25		1.25
Paracentral lobule	R	V		−0.16		0.79
Superior segment of the insula (posterior insula)	R	SA		−0.09		0.45
Superior occipital gyrus	L	V		−0.08		0.38
Temporal pole	R	MC		−0.08		0.42
Total gray matter	L/R	V		0.06		0.28

	Reward network
	Salience network
	Executive control network
	Emotional arousal
	Somatosensory network
	Thalamus
	Other (Regions not part of the reward, salience, executive control, emotional arousal, or somatosensory networks)

Abbreviations: Hemisphere: L, left, R, right. Morphometry metric: V, volume; SA, surface area; CT, cortical thickness; MC, mean curvature; Comp1: component 1; Comp2: component 2. Regions: OFG, orbital frontal gyrus; dlPFC, dorsal lateral prefrontal cortex; vmPFC, ventromedial prefrontal cortex; PCC, posterior parietal cortex; sgACC, subgenual anterior cingulate cortex; ACC, anterior cingulate cortex.

The components are referred to as brain signatures.

Loading is the measure of relative importance of the variables for the discrimination into the two groups for each brain signature.

Negative loadings for each component are associated with higher morphometric values in the overweight group compared to the normal weight group.

Positive loadings for each component are associated with lower morphometric values in the overweight group compared to the normal weight group.

Variable importance in projection (VIP) is a weighted sum of the loadings, which takes into account the explained variance of each brain signature. The averaged of the squared VIP scores is equal to 1.

[a]Reward network.

[b]Salience network.

[c]Executive control network.

[d]Emotional arousal.

[e]Somatosensory network.

[f]Thalamus.

[g]Other (regions not part of the reward, salience, executive control, emotional arousal, or somatosensory networks).

coefficients observed in brain signature 1 in that they included regions of the reward (caudate), salience (anterior insula), executive control (parts of the posterior parietal cortex), emotional arousal (parahippocampal gyrus, subgenual anterior cingulate cortex, and anterior cingulate cortex) and somatosensory (posterior insula and paracentral lobule) networks. However, brain signature 2 compared to brain signature 1 had only one connection from the reward network and more connections from regions of the salience and emotional arousal networks.

In overweight individuals compared to normal weight individuals, *lower* values for morphometry in the reward, salience, executive control and emotional arousal networks, but *higher* values in the somatosensory network were indicated.

4.0. Discussion

The aim of this study was to determine if morphological and anatomical patterns of brain connectivity (based on fiber density between specific brain regions) can discriminate overweight individuals from normal weight individuals. The main findings are: 1. Anatomical connectivity (relative density of white-matter tracts between regions) was able to discriminate between subjects with different BMI with high sensitivity (97%) and specificity (87%). 2. In contrast, morphological changes in gray-matter had a less than optimal classification accuracy. 3. Many of the brain regions comprising the discriminatory brain signatures belonged to the extended reward, salience, central executive, and emotional arousal networks suggesting that

functional impairments observed were due to abnormal organization between these networks.

4.1. Anatomical-connectivity based brain signatures associated with BMI

In this study, a classification algorithm consisting of two brain signatures reflecting distinct patterns of region connectivity showed a marked ability to discriminate between overweight individuals and normal weight individuals. Most DTI studies in high BMI individuals (Shott et al., 2014; Stanek et al., 2011; Xu et al., 2013; Yau et al., 2010, 2014) have focused on examining differences in white matter diffusion characteristics including fractional anisotropy and mean diffusivity (which measures integrity of white-matter tracts), or apparent diffusion coefficients (which measures water diffusion in the tracks and reflects cell damage). All these measures can provide information regarding localized changes in white-matter microstructure. In the current study we have focused on DTI measures of fiber tract density as a measure of estimating the relative connectivity between brain regions and networks. So, while other studies have localized changes within the white-matter microstructure, they have not identified the implications of these changes in terms of connectivity.

4.1.1. Anatomical connectivity based brain signature 1

The first brain signature was largely comprised by connections within and between reward, salience, executive control, emotional arousal, and sensory networks. There were also thalamic connections to regions of the executive control network and to the occipital region. Corresponding to our finding of decreased connections from the ventromedial prefrontal cortex to the anterior insula observed in the overweight group compared to the normal weight group, reduced integrity of white-matter tracts (reduced fractional anisotropy) in the external capsule (which contains fibers that connect cortical areas to other cortical areas via short association fibers) have been reported in obese compared to controls (Shott et al., 2014). Additionally, in obese compared to controls the apparent diffusion coefficient (water diffusion reflecting cell damage) was greater in the sagittal stratum (which is known for transmitting information from the parietal, occipital, cingulate and temporal regions to the thalamus), and may be consistent with our observations of lower connectivity between the right thalamus and the right middle occipital gyrus for overweight individuals compared to normal weight individuals (Shott et al., 2014). Shott and colleagues (Shott et al., 2014) also identified greater apparent diffusion coefficients (reflecting possible cell damage) in the obese group in the corona radiata, which appears to compliment our findings of lower relative fiber density between deep gray-matter structures (such as the thalamus) and cortical areas (dorsal lateral prefrontal cortex) in overweight individuals compared to normal weight individuals. Altered thalamic connectivity may interfere with the thalamus' role in facilitating the relay of peripheral sensory information to the cortex (Jang et al., 2014).

A separate study comparing uncomplicated adolescent obese to normal weight individuals also found reduced fractional anisotropy in obese adolescents in regions such as the external capsule, internal capsule (which mostly carries ascending and descending corticospinal tracts), as well as some temporal fibers and optic radiation (Yau et al., 2014). A recent study also observed loss of nerve fibers connections with DTI between the brainstem and hypothalamus in an individual with a brainstem cavernoma who, after undergoing surgical drainage, had a dramatic increase in weight, which may suggest that these nerve fibers are involved in the regulation of both food intake and weight (Purnell et al., 2014). However, we did not identify connectivity differences with the hypothalamus, which may in part be due to parcellation limitations based on the particular atlases used in the current study.

4.1.2. Anatomical connectivity based brain signature 2

A second orthogonal signature was comprised by only three anatomical connections within the reward and emotional arousal networks. The identification of altered connections within regions comprising the reward network and with regions in the networks it interacts with in the current study have not been previously reported. However, these alterations might be anticipated based on recent morphological studies that have observed gray matter alterations within regions of the extended reward network (Kenny, 2011; Kurth et al., 2013; Raji et al., 2010; Volkow et al., 2008). Together, our findings appear to show wide-spread alterations in white-matter connectivity for regions that comprise the reward network and its associated networks.

While other studies have found reduced fiber integrity as measured by reduced fractional anisotropy in regions of the corpus callosum and fornix (which are part of the cingulate and carry information from the hippocampus to the hypothalamus) with increasing BMI (Stanek et al., 2011; Xu et al., 2013); the current study did not identify significant alterations in interhemispheric connectivity within the two anatomical-connectivity brain signatures. The exception was that there was a connection between the left paracentral lobule and the right subparietal sulcus in brain signature 1, and a connection between the right putamen and the left gyrus rectus in brain signature 2. We hypothesize that the effect observed in these previous studies may be due to systemic white matter degradation instead of changes in connections between specific brain regions, similar to changes that occur during normal aging (Sullivan et al., 2010). While the authors of these previous studies hypothesized that differences in fractional anisotropy in the external capsule of subjects with high BMI may be correlated with connections from the hippocampus and amygdala, we did not observe significant changes in the connectivity within these structures. A more detailed analysis and finer parcellation of these brain regions are required to confirm these observations.

4.2. Morphometric gray-matter brain signatures associated with BMI

Gray matter morphometric analysis using two distinct profiles was able to correctly identify overweight from normal weight individuals with a sensitivity of 69% and a specificity of 63%. These findings are consistent with previous reports of global, and regional reductions in gray-matter volume in specific brain regions within the reward network and associated networks (Debette et al., 2010; Kenny, 2011; Kurth et al., 2013; Pannacciulli et al., 2006; Raji et al., 2010). In contrast to the DTI based classification, these findings suggest a moderate ability to discriminate between the two BMI groups.

4.2.1. Morphological based brain signature 1

In our study, the first brain signature displayed lower values of various morphometric measures (including subregions of the orbital frontal gyrus, anterior insula) in regions of the reward, salience, and executive control networks in the overweight group compared to the normal weight group. Additionally lower values morphometric values were observed for the inhibitory regions (dorsal lateral and ventromedial prefrontal cortex) related to the emotional arousal network, but higher morphometry for somatosensory network (precentral sulcus, supramarginal gyrus, subcentral sulcus, and superior frontal sulcus) including the temporal regions in overweight individuals compared to normal weight individuals. In this study we found significant reductions in morphological measurements (gray matter volume and cortical thickness) of the orbital frontal gyrus. The orbital frontal gyrus is an important region within the reward network which plays a role in evaluative processing and in the guidance of future behavior and decisions based on encoding anticipation related to reward (Kahnt et al., 2010). A recent study analyzing gray and white-matter structure found that obese individuals had reduced values for various regions within the reward network, including the orbital frontal gyrus (Shott et al., 2014).

4.2.2. Morphological based brain signature 2

Compared to brain signature 1, morphological measurements observed in regions of the salience and emotional arousal networks explained a majority of the variance, while the reward network regions were not influential. Reduced gray matter measurements were observed in regions of the salience, executive control and emotional arousal network. These regions (anterior insula, parietal posterior cortex, parahippocampal gyrus, subregions of the anterior cingulate cortex) are frequently associated with increased evoked brain activity during exposure to food cues (Brooks et al., 2013; Greenberg et al., 2006; Rothemund et al., 2007; Shott et al., 2014; Stoeckel et al., 2008), and degree of personal salience of stimuli (Critchley et al., 2011; Seeley et al., 2007a). In the current study, gray matter reductions were also seen in key regions of the somatosensory network (posterior insula, paracentral lobule). Even though the exact role of this network in overweight and obesity is not known, it has been shown to be involved in awareness of body sensations, and a recent study suggested that elevated somatosensory network activity in response to food cues in obese individuals could lead to overeating (Stice et al., 2011). This study specifically focused on morphological measurements and anatomical connections between brain regions in the extended reward network and somatosensory network, and suggests that these brain structural metrics may influence neural processing associated with the outcomes from functional studies found in the literature. Correlations with behavioral and environmental factors also offer further insight into the relationship between structural and functional findings, which will have to be tested in future studies.

4.3. The use of multivariate pattern analyses using sPLS-DA to discriminate between overweight and normal weight individuals

The findings about BMI related changes in fiber density between different brain networks within the extended reward network, support the hypothesis that increasing BMI results in disrupted anatomical connectivity between specific regions in the brain. These anatomical alterations may imply ineffective or inefficient communication between key regions of the reward network and related networks. Similar to several recent reports that have found overweight and obesity related changes in gray-matter volume (Debette et al., 2010; Kurth et al., 2013; Pannacciulli et al., 2006; Raji et al., 2010), we were also able to find similar morphological differences in overweight compared to normal weight individuals. In the current study, we extended these observations in order to investigate the association between overweight status and anatomical connectivity of the brain, and applied sPLS-DA to brain morphometric data to discriminate between overweight and normal weight subjects. A recent cross-sectional study using binary logistic regression suggests that the combination of structural changes in the lateral orbital frontal gyrus, as measured by gray-matter volume, and blood levels of an inflammatory marker (fibrinogen) was able to predict obesity in a small sample of 19 normal weight subjects and 44 overweight/obese subjects; with a high sensitivity (95.5%), but low specificity (31.6%) (Cazettes et al., 2011). Our study differs from this report in several aspects, including larger sample size; the use of a cross-validation approach to avoid a sample specific solution, exclusion of subjects with hypertension/diabetes mellitus to remove a possible confounder, and inclusion of both gray matter volume and fiber tract density to predict overweight status.

4.4. Limitations

Even though we found significant differences between individuals with normal weight and overweight in fiber density, we cannot extrapolate from these anatomic findings to differences in functional (resting state) connectivity. Such functional connectivity findings would offer the ability to detect differences in the synchronization of brain activity in areas that are not directly connected by white-matter tracts. Although we replicated previously reported findings about anatomical connectivity and morphological differences between overweight/obese and normal BMI (Kurth et al., 2013; Raji et al., 2010), we failed to observe alterations in important subcortical regions hypothalamus, amygdala, and hippocampus. It is possible that this failure may have been due to the limits of the automatic parcellation algorithms used in this study or due the analyses limited to overweight individuals versus obese individuals. Future studies would need larger samples in order to compare obese, overweight, and normal weight individuals, and to be able to conduct subgroup analyses based on sex and race. Due to our relatively small sample we employed a rigorous internal validation procedure, however, it remains necessary to test the predictive accuracy of this classifier in an independent data set (Bray et al., 2009). Future studies should address the association of these neuroimaging differences with specific eating behaviors, eating preferences, and diet information in order to interpret the context and significance of these findings. Since obesity and overweight status are often associated with comorbidities such hypertension, diabetes and metabolic syndrome, future analyses should investigate the moderating and correlation effects of these factors on the classification algorithm.

4.5. Summary and conclusions

In summary, our results support the hypothesis that being overweight is associated with altered connectivity (in the form of fiber density) between specific regions in the brain, which may imply ineffective or inefficient communication between these regions. In particular, the reduced connectivity of prefrontal inhibitory brain regions with the reward circuitry is consistent with a predominance of hedonic mechanisms in the regulation of food intake (Gunstad et al., 2006, 2007, 2008, 2010). The mechanisms underlying these structural changes are poorly understood, but may involve neuroinflammatory and neuroplastic processes (Cazettes et al., 2011) related to the low grade inflammatory state reported in overweight and obese individuals (Cazettes et al., 2011; Cox et al., 2014; Das, 2010; Gregor and Hotamisligil, 2011; Griffin, 2006). Data driven approaches to identify gray and white-matter alterations in overweight/obesity are promising tools to identify the central correlates of increasing BMI and have the potential to identify neurobiological biomarkers for this disorder.

Author contributions

Arpana Gupta: Study concept and design, analysis and interpretation of data, drafting and revision of manuscript.

Emeran Mayer: Study concept and design, critical review of manuscript, approval of the final version of manuscript, funding.

Claudia San Miguel: Drafting and critical review of manuscript, interpretation of data.

John Van Horn: Generation of data, analysis of data.

Connor Fling: Analysis of data.

Aubrey Love: Analysis of data.

Davis Woodworth: Analysis of data.

Benjamin Ellingson: Review of manuscript.

Kirsten Tillisch: Critical review of manuscript, funding.

Jennifer Labus: Study concept and design, analysis and interpretation of data, drafting and revision of the manuscript, approval of the final version of manuscript, funding.

Conflicts of interest

No conflicts of interest exist.

Source of funding

This research was supported in part by grants from the National Institutes of Health: R01 DK048351 (EAM), P50DK64539 (EAM), R01

AT007137 (KT), P30 DK041301, K08 DK071626 (JSL), and R03 DK084169 (JSL). Pilot scans were provided by the Ahmanson-Lovelace Brain Mapping Center, UCLA.

References

Bray, S., Chang, C., Hoeft, F., 2009. Applications of multivariate pattern classification analyses in developmental neuroimaging of healthy and clinical populations. Front. Hum. Neurosci. 3, 32. http://dx.doi.org/10.3389/neuro.09.032.200919893761.

Brooks, S.J., Cedernaes, J., Schiöth, H.B., 2013. Increased prefrontal and parahippocampal activation with reduced dorsolateral prefrontal and insular cortex activation to food images in obesity: a meta-analysis of fMRI studies. PLOS ONE 8 (4), e60393. http://dx.doi.org/10.1371/journal.pone.006039323593210.

Calton, M.A., Vaisse, C., 2009. Narrowing down the role of common variants in the genetic predisposition to obesity. Genome Med. 1 (3), 31. http://dx.doi.org/10.1186/gm3119341502.

Cazettes, F., Cohen, J.I., Yau, P.L., Talbot, H., Convit, A., 2011. Obesity-mediated inflammation may damage the brain circuit that regulates food intake. Brain Res. 1373, 101–109. http://dx.doi.org/10.1016/j.brainres.2010.12.00821146506.

Center for Disease Control (CDC), 2014. Overweight and Obesity I.

Chiang, M.C., Barysheva, M., Toga, A.W., Medland, S.E., Hansell, N.K., James, M.R., McMahon, K.L., de Zubicaray, G.I., Martin, N.G., Wright, M.J., Thompson, P.M., 2011. BDNF gene effects on brain circuitry replicated in 455 twins. Neuroimage 55 (2), 448–454.

Choquet, H., Meyre, D., 2011. Genetics of obesity: what have we learned? Curr. Genomics 12 (3), 169–179. http://dx.doi.org/10.2174/13892021179567789522043165.

Connolly, L., Coveleskie, K., Kilpatrick, L.A., Labus, J.S., Ebrat, B., Stains, J., Jiang, Z., Tillisch, K., Raybould, H.E., Mayer, E.A., 2013. Differences in brain responses between lean and obese women to a sweetened drink. Neurogastroenterol. Motil. 25 (7), 579-e460. http://dx.doi.org/10.1111/nmo.1212523566308.

Cox, A.J., West, N.P., Cripps, A.W., 2014. Obesity, inflammation, and the gut microbiota. Lancet Diabetes Endocrinol. http://dx.doi.org/10.1016/S2213-8587(14)70134-225066177.

Critchley, H.D., Nagai, Y., Gray, M.A., Mathias, C.J., 2011. Dissecting axes of autonomic control in humans: insights from neuroimaging. Auton. Neurosci. 161 (1–2), 34–42. http://dx.doi.org/10.1016/j.autneu.2010.09.00520926356.

Dale, A.M., Fischl, B., Sereno, M.I., 1999. Cortical surface-based analysis. I. Segmentation and surface reconstruction. Neuroimage 9 (2), 179–194. http://dx.doi.org/10.1006/nimg.1998.03959931268.

Das, U.N., 2010. Obesity: genes, brain, gut, and environment. Nutrition 26 (5), 459–473. http://dx.doi.org/10.1016/j.nut.2009.09.02020022465.

Debette, S., Beiser, A., Hoffmann, U., Decarli, C., O'Donnell, C.J., Massaro, J.M., Au, R., Himali, J.J., Wolf, P.A., Fox, C.S., Seshadri, S., 2010. Visceral fat is associated with lower brain volume in healthy middle-aged adults. Ann. Neurol. 68 (2), 136–144. http://dx.doi.org/10.1002/ana.2206220695006.

Destrieux, C., Fischl, B., Dale, A., Halgren, E., 2010. Automatic parcellation of human cortical gyri and sulci using standard anatomical nomenclature. Neuroimage 53 (1), 1–15. http://dx.doi.org/10.1016/j.neuroimage.2010.06.01020547229.

Dubois, L., Ohm Kyvik, K., Girard, M., Tatone-Tokuda, F., Pérusse, D., Hjelmborg, J., Skytthe, A., Rasmussen, F., Wright, M.J., Lichtenstein, P., Martin, N.G., 2012. Genetic and environmental contributions to weight, height, and BMI from birth to 19 years of age: an international study of over 12,000 twin pairs. PLOS ONE 7 (2), e30153. http://dx.doi.org/10.1371/journal.pone.003015322347368.

El-Sayed Moustafa, J.S., Froguel, P., 2013. From obesity genetics to the future of personalized obesity therapy. Nat. Rev. Endocrinol. 9 (7), 402–413. http://dx.doi.org/10.1038/nrendo.2013.5723529041.

Finkelstein, E.A., Trogdon, J.G., Cohen, J.W., Dietz, W., 2009. Annual medical spending attributable to obesity: payer- and service-specific estimates. Health Aff (Millwood) 28 (5), w822–w831. http://dx.doi.org/10.1377/hlthaff.28.5.w82219635784.

Fischl, B., Salat, D.H., Busa, E., Albert, M., Dieterich, M., Haselgrove, C., van der Kouwe, A., Killiany, R., Kennedy, D., Klaveness, S., Montillo, A., Makris, N., Rosen, B., Dale, A.M., 2002. Whole brain segmentation: automated labeling of neuroanatomical structures in the human brain. Neuron 33 (3), 341–355. http://dx.doi.org/10.1016/S0896-6273(02)00569-X11832223.

Fischl, B., Sereno, M.I., Dale, A.M., 1999. Cortical surface-based analysis. II: inflation, flattening, and a surface-based coordinate system. Neuroimage 9 (2), 195–207. http://dx.doi.org/10.1006/nimg.1998.03969931269.

García-García, I., Jurado, M.Á, Garolera, M., Segura, B., Sala-Llonch, R., Marqués-Iturria, I., Pueyo, R., Sender-Palacios, M.J., Vernet-Vernet, M., Narberhaus, A., Ariza, M., Junqué, C., 2013. Alterations of the salience network in obesity: a resting-state fMRI study. Hum. Brain Mapp. 34 (11), 2786–2797. http://dx.doi.org/10.1002/hbm.2210422522963.

Greenberg, J.A., Boozer, C.N., Geliebter, A., 2006. Coffee, diabetes, and weight control. Am. J. Clin. Nutr. 84 (4), 682–69317023692.

Gregor, M.F., Hotamisligil, G.S., 2011. Inflammatory mechanisms in obesity. Annu. Rev. Immunol. 29, 415–445. http://dx.doi.org/10.1146/annurev-immunol-031210-10132221219177.

Griffin, W.S., 2006. Inflammation and neurodegenerative diseases. Am. J. Clin. Nutr. 83 (2), 470S–474S16470015.

Gunstad, J., Lhotsky, A., Wendell, C.R., Ferrucci, L., Zonderman, A.B., 2010. Longitudinal examination of obesity and cognitive function: results from the Baltimore longitudinal study of aging. Neuroepidemiology 34 (4), 222–229. http://dx.doi.org/10.1159/00029774220299802.

Gunstad, J., Paul, R.H., Cohen, R.A., Tate, D.F., Gordon, E., 2006. Obesity is associated with memory deficits in young and middle-aged adults. Eat. Weight Disord. 11 (1), e15–e19. http://dx.doi.org/10.1007/BF03327747716801734.

Gunstad, J., Paul, R.H., Cohen, R.A., Tate, D.F., Spitznagel, M.B., Gordon, E., 2007. Elevated body mass index is associated with executive dysfunction in otherwise healthy adults. Compr. Psychiatry 48 (1), 57–61. http://dx.doi.org/10.1016/j.comppsych.2006.05.00117145283.

Gunstad, J., Spitznagel, M.B., Paul, R.H., Cohen, R.A., Kohn, M., Luyster, F.S., Clark, R., Williams, L.M., Gordon, E., 2008. Body mass index and neuropsychological function in healthy children and adolescents. Appetite 50 (2–3), 246–251. http://dx.doi.org/10.1016/j.appet.2007.07.00817761359.

Irimia, A., Chambers, M.C., Torgerson, C.M., Van Horn, J.D., 2012. Circular representation of human cortical networks for subject and population-level connectomic visualization. Neuroimage 60 (2), 1340–1351. http://dx.doi.org/10.1016/j.neuroimage.2012.01.10722305988.

Jang, S.H., Lim, H.W., Yeo, S.S., 2014. The neural connectivity of the intralaminar thalamic nuclei in the human brain: a diffusion tensor tractography study. Neurosci. Lett. 579, 140–144. http://dx.doi.org/10.1016/j.neulet.2014.07.02425058432.

Kahnt, T., Heinzle, J., Park, S.Q., Haynes, J.D., 2010. The neural code of reward anticipation in human orbitofrontal cortex. Proc. Natl. Acad. Sci. U S A 107 (13), 6010–6015. http://dx.doi.org/10.1073/pnas.091283810720231475.

Kenny, P.J., 2011. Reward mechanisms in obesity: new insights and future directions. Neuron 69 (4), 664–679. http://dx.doi.org/10.1016/j.neuron.2011.02.01621338878.

Kilpatrick, L.A., Coveleskie, K., Connolly, L., Labus, J.S., Ebrat, B., Stains, J., Jiang, Z., Suyenobu, B.Y., Raybould, H.E., Tillisch, K., Mayer, E.A., 2014. Influence of sucrose ingestion on brainstem and hypothalamic intrinsic oscillations in lean and obese women. Gastroenterology 146 (5), 1212–1221. http://dx.doi.org/10.1053/j.gastro.2014.01.02324480616.

Kullmann, S., Heni, M., Veit, R., Ketterer, C., Schick, F., Häring, H.U., Fritsche, A., Preissl, H., 2012. The obese brain: association of body mass index and insulin sensitivity with resting state network functional connectivity. Hum. Brain Mapp. 33 (5), 1052–1061. http://dx.doi.org/10.1002/hbm.2126821520345.

Kurth, F., Levitt, J.G., Phillips, O.R., Luders, E., Woods, R.P., Mazziotta, J.C., Toga, A.W., Narr, K.L., 2013. Relationships between gray matter, body mass index, and waist circumference in healthy adults. Hum. Brain Mapp. 34 (7), 1737–1746. http://dx.doi.org/10.1002/hbm.2202122419507.

Lê Cao, K.A., Boitard, S., Besse, P., 2011. Sparse PLS discriminant analysis: biologically relevant feature selection and graphical displays for multiclass problems. BMC Bioinformatics 12, 253. http://dx.doi.org/10.1186/1471-2105-12-25321693065.

Lê Cao, K.A., González, I., Déjean, S., 2009a. integrOmics: an R package to unravel relationships between two omics datasets. BioInformatics 25 (21), 2855–2856. http://dx.doi.org/10.1093/bioinformatics/btp51519706745.

Lê Cao, K.A., Martin, P.G., Robert-Granié, C., Besse, P., 2009b. Sparse canonical methods for biological data integration: application to a cross-platform study. BMC Bioinformatics 10, 34. http://dx.doi.org/10.1186/1471-2105-10-3419171069.

Lê Cao, K.A., Rossouw, D., Robert-Granié, C., Besse, P., 2008a. A sparse PLS for variable selection when integrating omics data. Stat. Appl. Genet. Mol. Biol. 7 (1), 35. http://dx.doi.org/10.2202/1544-6115.139019049491.

Lê Cao, K.A., Rossouw, D., Robert-Granié, C., Besse, P., 2008b. A sparse PLS for variable selection when integrating omics data. Stat. Appl. Genet. Mol. Biol. 7 (1), 35. http://dx.doi.org/10.2202/1544-6115.139019049491.

Loveman, E., Frampton, G.K., Shepherd, J., Picot, J., Cooper, K., Bryant, J., Welch, K., Clegg, A., 2011. The clinical effectiveness and cost-effectiveness of long-term weight management schemes for adults: a systematic review. Health Technol. Assess. 15 (2), 1–182. http://dx.doi.org/10.3310/hta1502021247515.

Menon, V., Uddin, L.Q., 2010. Saliency, switching, attention and control: a network model of insula function. Brain Struct. Funct. 214 (5–6), 655–667. http://dx.doi.org/10.1007/s00429-010-0262-020512370.

Mori, S., Crain, B.J., Chacko, V.P., van Zijl, P.C., 1999. Three-dimensional tracking of axonal projections in the brain by magnetic resonance imaging. Ann. Neurol. 45 (2), 265–269. http://dx.doi.org/10.1002/1531-8249(199902)45:2<265::AID-ANA21>3.0.CO;2-39989633.

Morrow, J.D., Maren, S., Robinson, T.E., 2011. Individual variation in the propensity to attribute incentive salience to an appetitive cue predicts the propensity to attribute motivational salience to an aversive cue. Behav. Brain Res. 220 (1), 238–243. http://dx.doi.org/10.1016/j.bbr.2011.02.01321316397.

Pannacciulli, N., Del Parigi, A., Chen, K., Le, D.S., Reiman, E.M., Tataranni, P.A., 2006. Brain abnormalities in human obesity: a voxel-based morphometric study. Neuroimage 31 (4), 1419–1425. http://dx.doi.org/10.1016/j.neuroimage.2006.01.04716545583.

Purnell, J.Q., Lahna, D.L., Samuels, M.H., Rooney, W.D., Hoffman, W.F., 2014. Loss of pons-to-hypothalamic white matter tracks in brainstem obesity. Int J Obes (Lond) 38, 1573–1577. http://dx.doi.org/10.1038/ijo.2014.5724727578.

Raji, C.A., Ho, A.J., Parikshak, N.N., Becker, J.T., Lopez, O.L., Kuller, L.H., Hua, X., Leow, A.D., Toga, A.W., Thompson, P.M., 2010. Brain structure and obesity. Hum. Brain Mapp. 31 (3), 353–364. http://dx.doi.org/10.1002/hbm.2087019662657.

Rothemund, Y., Preuschhof, C., Bohner, G., Bauknecht, H.C., Klingebiel, R., Flor, H., Klapp, B.F., 2007. Differential activation of the dorsal striatum by high-calorie visual food stimuli in obese individuals. Neuroimage 37 (2), 410–421. http://dx.doi.org/10.1016/j.neuroimage.2007.05.00817566768.

Seeley, W.W., Menon, V., Schatzberg, A.F., Keller, J., Glover, G.H., Kenna, H., Reiss, A.L., Greicius, M.D., 2007a. Dissociable intrinsic connectivity networks for salience processing and executive control. J. Neurosci. 27 (9), 2349–2356. http://dx.doi.org/10.1523/JNEUROSCI.5587-06.200717329432.

Seeley, W.W., Menon, V., Schatzberg, A.F., Keller, J., Glover, G.H., Kenna, H., Reiss, A.L., Greicius, M.D., 2007b. Dissociable intrinsic connectivity networks for salience

processing and executive control. J. Neurosci. 27 (9), 2349–2356. http://dx.doi.org/10.1523/JNEUROSCI.5587-06.200717329432.
Sheehan, D.V., Lecrubier, Y., Sheehan, K.H., Amorim, P., Janavs, J., Weiller, E., Hergueta, T., Baker, R., Dunbar, G.C., 1998. The Mini-International Neuropsychiatric Interview (M.I.N.I.): the development and validation of a structured diagnostic psychiatric interview for DSM-IV and ICD-10. J. Clin. Psychiatry 59 (Suppl. 20), 22–339881538 [Quiz 34–57].
Shott, M.E., Cornier, M.A., Mittal, V.A., Pryor, T.L., Orr, J.M., Brown, M.S., Frank, G.K., 2014. Orbitofrontal cortex volume and brain reward response in obesity. Int J Obes (Lond) http://dx.doi.org/10.1038/ijo.2014.12125027223.
Stanek, K.M., Grieve, S.M., Brickman, A.M., Korgaonkar, M.S., Paul, R.H., Cohen, R.A., Gunstad, J.J., 2011. Obesity is associated with reduced white matter integrity in otherwise healthy adults. Obesity (Silver Spring) 19 (3), 500–504. http://dx.doi.org/10.1038/oby.2010.31221183934.
Stice, E., Yokum, S., Burger, K.S., Epstein, L.H., Small, D.M., 2011. Youth at risk for obesity show greater activation of striatal and somatosensory regions to food. J. Neurosci. 31 (12), 4360–4366. http://dx.doi.org/10.1523/JNEUROSCI.6604-10.201121430137.
Stoeckel, L.E., Weller, R.E., Cook 3rd, E.W., Twieg, D.B., Knowlton, R.C., Cox, J.E., 2008. Widespread reward-system activation in obese women in response to pictures of high-calorie foods. Neuroimage 41 (2), 636–647. http://dx.doi.org/10.1016/j.neuroimage.2008.02.03118413289.
Sullivan, E.V., Rohlfing, T., Pfefferbaum, A., 2010. Longitudinal study of callosal microstructure in the normal adult aging brain using quantitative DTI fiber tracking. Dev. Neuropsychol. 35 (3), 233–256. http://dx.doi.org/10.1080/87565641003689556204461 31.
Terranova, L., Busetto, L., Vestri, A., Zappa, M.A., 2012. Bariatric surgery: cost-effectiveness and budget impact. Obes. Surg. 22 (4), 646–653. http://dx.doi.org/10.1007/s11695-012-0608-122290621.
Volkow, N.D., Frascella, J., Friedman, J., Saper, C.B., Baldo, B., Rolls, E.T., Mennella, J.A., Dallman, M.F., Wang, G.J., LeFur, G., 2004. Neurobiology of obesity: relations to addiction. Neuropsychopharmacology 29, S29–S30.
Volkow, N.D., Wang, G.J., Baler, R.D., 2011. Reward, dopamine and the control of food intake: implications for obesity. Trends Cogn. Sci. 15 (1), 37–46. http://dx.doi.org/10.1016/j.tics.2010.11.00121109477.
Volkow, N.D., Wang, G.J., Fowler, J.S., Telang, F., 2008. Overlapping neuronal circuits in addiction and obesity: evidence of systems pathology. Philos. Trans. R. Soc. Lond., B, Biol. Sci. 363 (1507), 3191–3200. http://dx.doi.org/10.1098/rstb.2008.010718640912.
World Health Organization (WHO), 2014. Obesity I.
Xu, J., Li, Y., Lin, H., Sinha, R., Potenza, M.N., 2013. Body mass index correlates negatively with white matter integrity in the fornix and corpus callosum: a diffusion tensor imaging study. Hum. Brain Mapp. 34 (5), 1044–1052. http://dx.doi.org/10.1002/hbm.2149122139809.
Yau, P.L., Javier, D.C., Ryan, C.M., Tsui, W.H., Ardekani, B.A., Ten, S., Convit, A., 2010. Preliminary evidence for brain complications in obese adolescents with type 2 diabetes mellitus. Diabetologia 53 (11), 2298–2306. http://dx.doi.org/10.1007/s00125-010-1857-y20668831.
Yau, P.L., Kang, E.H., Javier, D.C., Convit, A., 2014. Preliminary evidence of cognitive and brain abnormalities in uncomplicated adolescent obesity. Obesity (Silver Spring) 22 (8), 1865–1871. http://dx.doi.org/10.1002/oby.2080124891029.
Zald, D.H., 2003. The human amygdala and the emotional evaluation of sensory stimuli. Brain Res. Brain Res. Rev. 41 (1), 88–123. http://dx.doi.org/10.1016/S0165-0173(02)00248-512505650.
Zigmond, A.S., Snaith, R.P., 1983. The hospital anxiety and depression scale. Acta Psychiatr. Scand. 67 (6), 361–370. http://dx.doi.org/10.1111/j.1600-0447.1983.tb09716.x6880820.